Modelling silicon supply during the Last Interglacial (MIS 5e) at Lake Baikal

Panizzo, V.N.[1,2], Swann, G.E.A.[1,2], Mackay, A.W.[3], Pashley, V.[4], and Horstwood, M.S.A.[4]

[1]*School of Geography, University of Nottingham, University Park, Nottingham, NG7 2RD, UK*

[2]*Centre for Environmental Geochemistry, University of Nottingham, University Park, Nottingham, NG7 2RD, UK*

[3]*Environmental Change Research Centre, Department of Geography, University College London, Gower Street, London, WC1E 6BT, UK*

[4]*NERC Isotope Geosciences Laboratory, British Geological Survey, Keyworth, Nottingham, NG12 5GG, UK*

*Corresponding author: virginia.panizzo@nottingham.ac.uk.

Abstract

Throughout the Quaternary, lake productivity has been shown to be sensitive to drivers such as climate change, landscape evolution and lake ontogeny. In particular, sediments from Lake Baikal, Siberia, provide a valuable uninterrupted and continuous sequence of palaeoproductivity, which document orbital and sub-orbital frequencies of regional climate change. Here we augment these records through the application of silicon stable isotope analyses of diatom opal ($\delta^{30}Si_{diatom}$), from sediments spanning the Last Interglacial cycle (approximately equivalent to Marine Isotope Stage [MIS] 5e; c. 130 to 115 ka BP) as a means to test the hypothesis that diatom nutrient utilisation was greater, than during the Holocene. Results show that diatom dissolved silicon (DSi) utilisation, was significantly greater ($p=0.001$) during MIS 5e than the current interglacial, which reflects increased diatom productivity over this time (concomitant with higher biogenic silica and warmer pollen-inferred vegetation reconstructions). Diatom biovolume accumulation rates (BVAR) are used, in tandem with $\delta^{30}Si_{diatom}$ data, to model DSi supply to Lake Baikal surface waters. When constrained by sedimentary mineralogical archives of catchment weathering indices (e.g. the Hydrolysis Index), data highlight the small degree of weathering intensity and therefore representation that catchment-weathering DSi sources had, over the duration of MIS 5e. Changes to DSi supply during the Last Interglacial are attributed to variations in within-lake conditions (e.g. turbulent mixing) over the period, where periods

of both high productivity and modeled-DSi supply (e.g. strong convective mixing) account for the decreasing trend in $\delta^{30}Si_{diatom}$ compositions (after c. 124 ka BP).

Key words

Last Interglacial, Kazantsevo, diatoms, silicon isotopes, Siberia, palaeoproductivity

1. Introduction:

Primary productivity is a key ecosystem function synthesizing organic matter, and in deep lakes production is usually dominated by phytoplankton. Over long timescales, primary production is controlled by a number of extrinsic drivers such as climate change, landscape evolution and lake ontogeny, although species composition also has an important influence on productivity-diversity relationships (e.g. Dodson et al., 2000). On Quaternary timescales palaeoproductivity may be estimated using a number of different techniques, including palaeoecological (e.g. diatom analysis) biogeochemical (e.g. biogenic silica or pigment analysis) and stable isotope approaches. Palaeoproductivity records allow us to test key hypotheses related to climate variability, including differences between interglacial periods, which may act as analogues to a future warming world. One of the most studied interglacials is the Last Interglacial, as a possible analogue for a future, warmer Earth (although in terms of orbital configuration, this comparison is imperfect).

The Last Interglacial, corresponding to Marine Isotope Stage (MIS) 5e (130 - 115 ka BP; PAGES, 2016; Railsback et al., 2015), is often referred to as the Eemian in Western European continental records or the Kazantsevo in southern Siberia. In order to more fully understand the nature, duration and synchroneity of MIS 5e across the globe, the comparison of independent continental and oceanic climate records are needed. Lake Baikal, Siberia (103°43'-109°58'E and 51°28'-55°47'N; Figure 1) provides a key uninterrupted, continental sedimentary archive, which spans at least the past 20 million years (Williams et al., 2001), to which further Eurasian continental records (e.g. loess sequences) can be compared (Prokopenko et al., 2006). Lake Baikal is the world’s deepest and most voluminous lake (23, 615 km^2) with a catchment of over 540, 000 km^2. Its mid-latitude location in central Asia means that the lake is highly continental (Lydolph, 1977), and sensitive to obliquity- and precessional-driven forcing (Short et al., 1991) which has allowed an astronomically tuned climate record for the entire Pleistocene (Prokopenko et al., 2006).

Figure 1.

Map of Lake Baikal and its catchment with core locations CON-01-603-2 and BDP-96 identified.

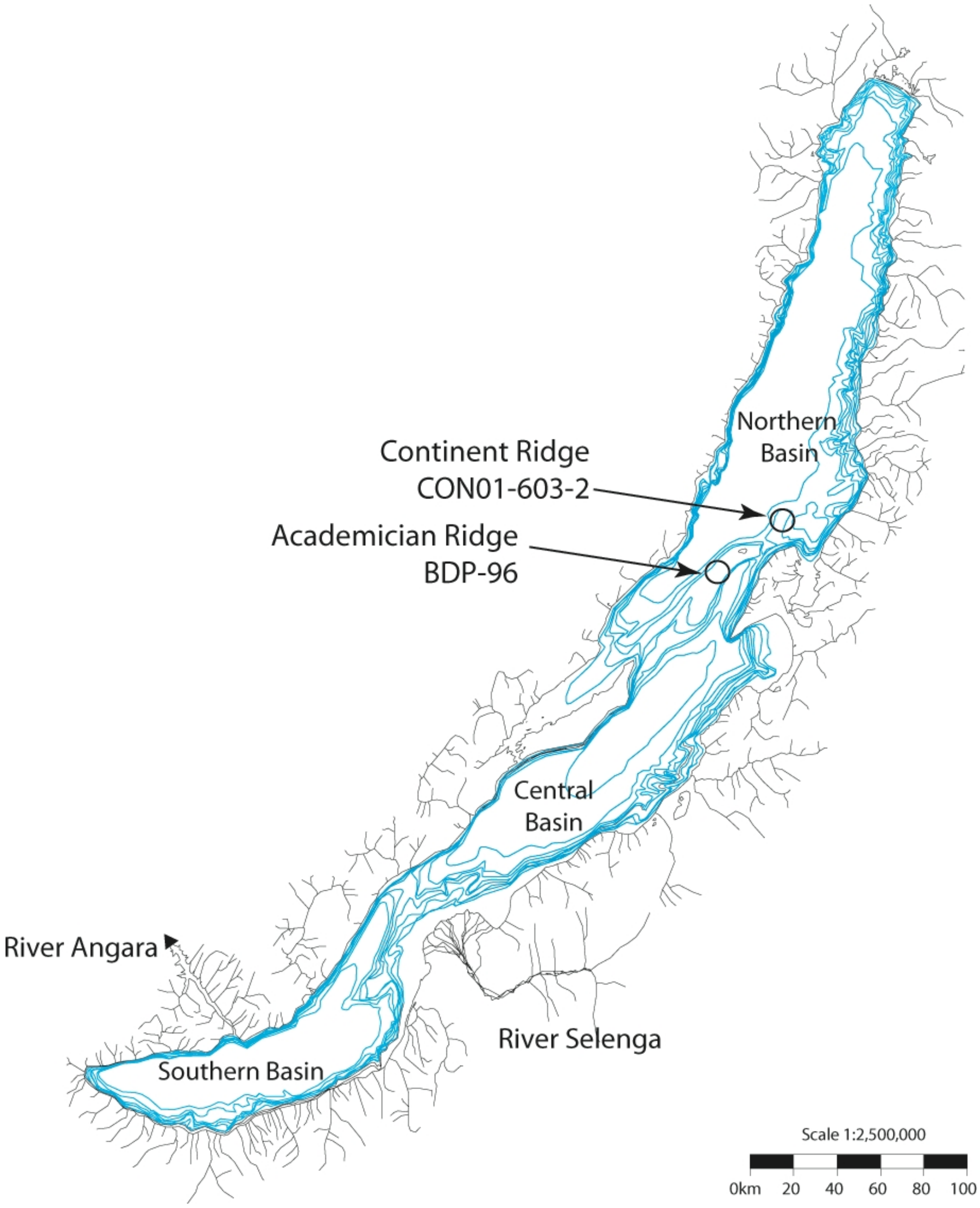

Prokopenko et al. (2001) argued that biogenic silica (BSi) records from Lake Baikal register regional climatic fluctuations (e.g. glacial-interglacial cycles), and are linked to incoming solar radiation (hereafter insolation) forcing, via heat balance exchanges within the lake (e.g. Prokopenko et al., 2006; Prokopenko et al., 2001). At sub-orbital frequencies, BSi concentration may be related to regional climate change, linked to teleconnections with shifting Atlantic Meridional Overturning Circulation (e.g. Karabanov et al., 2000). On orbital timescales, Lake Baikal BSi records are interpreted as a palaeoproductivity proxy (Mackay, 2007; Prokopenko et al., 2006; Prokopenko et al., 2001). Seasonal phytoplankton succession at Lake Baikal today is controlled by the timing of ice-off (end of May-June) and ice-on (after October), which promote a period of rapid diatom growth via upper water column turbulent mixing (Popovskaya, 2000). The thermal regime of Lake Baikal in spring and autumn periods is therefore very important in regulating diatom bloom development at these times, although the availability of dissolved silicon (DSi) is also significantly important (Panizzo et al., In review; Popovskaya et al., 2015). While these productivity proxies (e.g. BSi, in tandem with diatom assemblages) can provide an insight into variations in limnological characteristics (e.g. length of growing season, lake turnover) over previous glacial-interglacial cycles, they do not provide the ability to quantitatively assess variations between within-lake, versus catchment, delivery of nutrients (namely DSi). We aim to address this in this study, via the use of silicon stable isotope geochemistry to reconstruct such changes over the Last Intrglacial.

There are three stable isotopes of silicon (Si: ^{28}Si, ^{29}Si and ^{30}Si), which fractionate during almost all low-temperature processes of the continental and oceanic silicon cycles, highlighting their value as a geochemical tracer. Variations in the isotope abundances (e.g. $^{30}Si/^{28}Si$ [although previously more commonly $^{29}Si/^{28}Si$]) are reported via the delta notation ($\delta^{30}Si$), when compared to a known standard reference material (e.g. NBS 28). Records of $\delta^{30}Si$ composition of waters and diatom opal ($\delta^{30}Si_{DSi}$ and $\delta^{30}Si_{diatom}$ respectively) from Lake Baikal have demonstrated the clear relationship between diatom biomass and nutrient availability (Panizzo et al., In review; Panizzo et al., 2017; Panizzo et al., 2016), pointing to $\delta^{30}Si_{diatom}$ as a proxy for surface water DSi utilisation. This is as DSi (in the form of silicic acid [$Si(OH)_4$]), is a key nutrient for diatom uptake and growth (Martin-Jezequel et al., 2000). During biomineralisaton diatoms discriminate against the heavier isotopes (^{29}Si and ^{30}Si), over the lighter (^{28}Si), which leads to the preferential isotopic enrichment of the residual solution (in this case, the dissolved phase: $\delta^{30}Si_{DSi}$) in the heavier isotopes. This is turn leaves a clear biological imprint on the isotopic composition of BSi (De La Rocha et al., 1997). While the per mille fractionation or enrichment factor (termed $^{30}\varepsilon_{uptake}$) between both phases is considered to be between c. −1.1 and −1.6‰ (estimated from freshwater systems; Alleman et al., 2005; Opfergelt et al., 2011; Panizzo et al., 2016; Sun et al., 2013) and be independent of temperature, pCO$_2$ and nutrient availability (De La Rocha et al., 1997; Fripiat et al., 2011; Milligan et al., 2004; Varela et al., 2004) some *in-vitro* studies on oceanic diatoms have pointed to a species dependent $^{30}\varepsilon_{uptake}$ effect (Sutton et al., 2013). While this final attestation remains in dispute, in the case of Lake Baikal *in-situ* estimations of diatom $^{30}\varepsilon_{uptake}$ are c. -1.6‰, derived from calculations of seasonal BSi (Panizzo et al., 2016). A final important consideration is the preservation of the $\delta^{30}Si_{diatom}$ in surface sediments, where in Lake Baikal, it is estimated that only c. 1% of total diatom valves are preserved (Ryves et al., 2003). Nevertheless, Panizzo et al. (2016) demonstrate the absence of any diatom dissolution associated $^{30}\varepsilon$ (as per earlier studies by Demarest et al., 2009) and therefore validate the application of $\delta^{30}Si_{diatom}$ reconstructions from lake sediments.

On the basis of the above discussion and earlier work at Lake Baikal (Panizzo et al., In review; Panizzo et al., 2017; Panizzo et al., 2016), we propose that $\delta^{30}Si_{diatom}$ sedimentary records can act as a tracer of past diatom nutrient uptake. In addition, we here apply silicon isotope geochemistry from Lake Baikal sediments as a means to explore, in more detail, the catchment and within-lake constraints on silicon cycling (via the application of independent diatom productivity proxies), as a means to understand how climate has impacted nutrient supply, productivity and export at Lake Baikal over MIS 5e. Our objectives are to firstly provide an overview of $\delta^{30}Si_{diatom}$ signatures in MIS 5e and determine if diatom utilisation was greater than the current interglacial. Secondly, to reconstruct palaeo-nutrient supply of DSi in Lake Baikal surface waters over the course of the Last Interglacial. In particular, we compare these parameters with existing palaeolimnolgical proxies to better reconstruct variations in nutrient availability and diatom uptake, as a response to prevailing orbital and climatological changes. Finally we devise a new interpretive model to best describe intra-Last Interglacial variability at Lake Baikal.

2. Materials and methods:

2.1. Core collection

Core CON-01-603-2 was collected in the Continental Ridge, north basin, of Lake Baikal in July 2001 at the location of 53°57´ N, 108°54´ E (Figure 1). The core was collected from a water depth of 386 m using a piston corer, with full details provided by Demory et al. (2005a); Demory et al. (2005b) Charlet et al. (2005). Detailed summaries on CON-01-603-2 core collection, chronology formation (radiocarbon and palaeomagnetism) can be found therein. Here we present the methods for this new data set of $\delta^{30}Si_{diatom}$ alone, although reference is also made to existing datasets of $\delta^{18}O_{diatom}$ (Mackay et al., 2013), diatom biovolume accumulation rates (BVAR) (Rioual and Mackay, 2005), catchment weathering indices (e.g. sediment clay mineralogy; Fagel and Mackay, 2008) and pollen-derived vegetation biome reconstructions (Tarasov et al., 2005; derived from the pollen reconstructions of Granoszewski et al., 2005) from the same core (Figures 3,4).

2.2. Silicon isotope preparation and analysis

A total of 16 samples for $\delta^{30}Si_{diatom}$ analyses were selected across an existing $\delta^{18}O_{diatom}$ record (Mackay et al., 2013) from sediment core CON-01-603-2. Samples underwent further preparation to remove high episodes of contamination (namely Al_2O_3) via more vigorous cleaning (of the exisiting diatom opal from Mackay et al., 2013), including heavy density separation and organic material oxidation (as per methods outlined in Morley et al., 2004). Prior to isotopic analysis, all samples were visually inspected via a Zeiss Axiovert 40 C inverted microscope with X-ray fluorescence (XRF) analyses also conducted in order to quantitatively verify their purity. All samples demonstrated no visual contamination (e.g. clay) and quantitative estimations via XRF are <1% (with sample Al_2O_3/SiO_2 <0.01).

Alkaline fusion (NaOH) of cleaned diatom opal and subsequent ion-chromatography (via cation exchange methods; BioRad AG50W-X12) followed methodologies outlined by Georg et al. (2006), with further methodological practices mentioned in Panizzo et al. (2016). Samples were analysed in wet-plasma mode using the high mass-resolution capability of a ThermoScientific Neptune Plus MC-ICP-MS (multi collector inductively coupled plasma mass spectrometer) at the British Geological Survey. Full analytical methods are detailed in Panizzo et al. (2017); Panizzo et al. (2016), including practices applied to minimize instrument induced mass bias and drift (e.g. Cardinal et al., 2003; Hughes et al., 2011). Full procedural blank compositions from MC-ICP-MS analyses were c. 31 ng compared to typical fusion amounts of c. 3390 ng and differed from sample compositions by < 0.5%. Using the worst case scenario (i.e. calculated using the sample with the lowest Si concentration) this level of blank could result in a potential shift in sample composition by < 0.04‰. All blank measurements therefore demonstrated an insignificant effect relative to the typical <0.11‰ propagated sample uncertainties (Table 1) and no correction for procedural blank was made.

All uncertainties are reported at 2σ absolute (Table 1), and incorporate an excess variance derived from the NBS 28 reference material, which was quadratically added to the analytical uncertainty of each measurement. δ^{29}Si and δ^{30}Si were compared to the mass dependent fractionation line to which all samples comply (Figure 2). Long term (~ 2 years) reproducibility and machine accuracy are assessed via analyzing the Diatomite secondary standard and data agree with the published values: Diatomite = +1.24‰ ± 0.18‰ (2 SD, n=244) (consensus value of +1.26‰ ± 0.2‰, 2 SD; Reynolds et al., 2007).

Figure 2.
Three-isotope plot (δ^{29}Si vs δ^{30}Si) for all silicon isotope data (n=16) presented in this manuscript, with data falling within analytical uncertainty of the mass-dependent fractionation line (dashed).

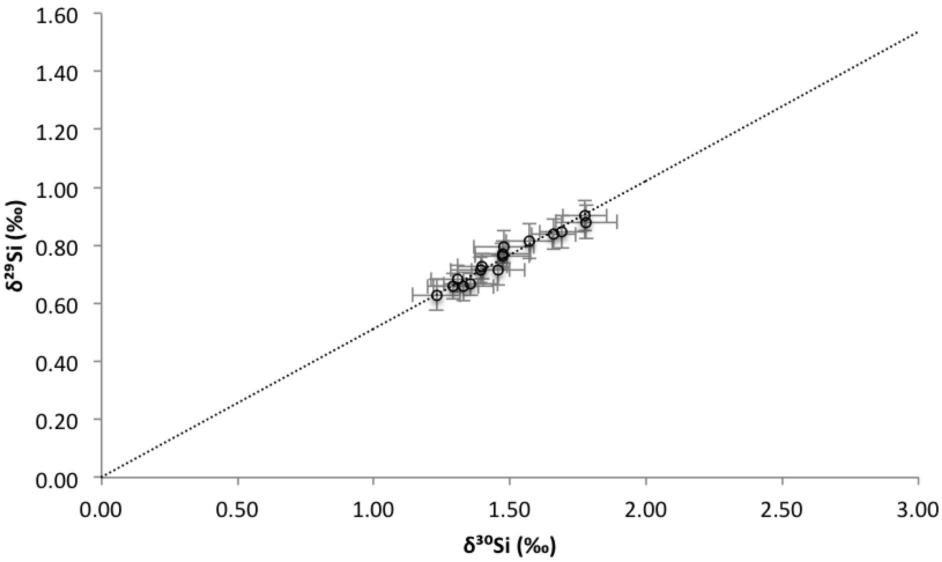

2.3. Modeling palaeo-surface water nutrient availability

Based on an open system model approach (Eq. 1), which is considered most appropriate at Lake Baikal (Panizzo et al. (2017), the equation can be re-arranged to calculate palaeo $\%DSi_{utilisation}$ (Eq. 2):

$$\delta^{30}Si_{DSi} = \delta^{30}Si_{initial} - {}^{30}\varepsilon_{uptake}\,(1 - f_{Si}) \qquad \text{Eq. 1}$$

$$\%DSi_{utilisation} = 1 - [(\delta^{30}Si_{diatom} - \delta^{30}Si_{initial} / -{}^{30}\varepsilon_{uptake}] \qquad \text{Eq. 2}$$

Where $\delta^{30}Si_{initial}$ is the initial composition of the dissolved pool, before biological enrichment. This is set here at +1.71‰ based on modern day south basin deep water (>400m) compositions from Lake Baikal, which we argue act as baseline surface water compositions when ice-off and turbulent mixing occurs, leading to the first (larger) spring diatom bloom (Panizzo et al., 2017). The assumption that modern day $\delta^{30}Si_{initial}$ can be applied here may lead to some uncertainty in $\%DSi_{utilisation}$ estimations (e.g. >100%; Table 1) however, in the absence of palaeo-$\delta^{30}Si_{initial}$ compositions from Lake Baikal we argue its application here. $\delta^{30}Si_{diatom}$ is the isotopic composition of diatom opal at any given time interval and ${}^{30}\varepsilon_{uptake}$ is set at −1.6‰, as discussed in Section 1 (Panizzo et al., 2017; Panizzo et al., 2016).

In addition to simply quantifying past DSi surface utilisation via diatom biomineralisation, a further application is applied here. As independent diatom productivity indicators (e.g. BVAR) are also available from core CON-01-603-2, (Rioual and Mackay, 2005), an estimate of DSi supply can be made by constraining $\delta^{30}Si_{diatom}$ compositions by the net export of BSi to sediments (e.g. as a function of export production or nutrient demand; Horn et al., 2011). This application has been seen in oceanic settings as a method to better constrain reconstructions of nutrient supply, when coupled with other algal productivity indicators (Horn et al., 2011).

$$DSi\ Supply = \frac{F_{BVAR}^{sample} / F_{BVAR}^{120.5\ ka}}{\%DSi_{consumed}^{sample} / \%DSi_{consumed}^{120.5\ ka}} \qquad \text{Eq. 3}$$

F_{BVAR}^{sample} is the flux of BVAR in sediments and $\%DSi_{consumed}^{sample}$ is the percentage of the DSi consumed by diatoms (in the sediment record). $F_{BVAR}^{120.5\ ka}$ and $\%DSi_{consumed}^{120.5\ ka}$ are defined as the sample with the greatest modeled supply in the MIS 5e record (at c. 120.5 ka BP; Table 1). We apply the use of BVAR here (over %BSi) as we argue this reflects more realistically the DSi demand of diatoms. Diatom BVAR take into consideration diatom size (e.g. volume) and cell fluxes, and so the amount of DSi biomineralised in the valve (refer to Rioual and Mackay, 2005, for full explanation of calculation). BSi records on the other hand represent bulk biogenic opal in sediments, which has evaded remineralisation (e.g. Ryves et al., 2003) and may not be exclusively diatomaceous in origin (e.g. catchment derived amorphous silica). Zonation of Figure 4 and the discussion surrounding the conceptual model at Lake Baikal (Section 4.2; Figure 5) is based on the Diatom Assemblage Zonations (DAZ) defined by Rioual and Mackay (2005).

3. Results:

The data set presented here starts at the end of Termination 2 (c. 132 ka BP, n=1) through to the transition from MIS 5e to MIS 5d at c. 116 ka BP. The resolution of sampling is at the millennial-scale, c. every 850 years. All $\delta^{30}Si_{diatom}$ data range between +1.23 and +1.78‰ (0.17‰ 1SD of all final data, n=16; Table 1). Lowest $\delta^{30}Si_{diatom}$ compositions are seen at c. 132.1 ka BP (+1.23 ± 0.09‰, n=1; Table 1), during zone MIS 6. Highest values (between +1.77 ± 0.08‰ and +1.48 ± 0.11‰, n=7; Table 1) are demonstrated in early MIS 5e (c. 127.4 and 123.0 ka BP), with a progression to lower values (c. 1.47 ± 0.1‰ and +1.30 ± 0.10, n=8; Table 1) between c. 122.0 and 116.1 ka BP (Figure 3). There is one episode of lower signatures, outside of the general MIS 5e decreasing trend, between c. 127.4 and 126.8 ka BP, where values fall to +1.46 ± 0.1‰ (at c. 126.8 ka BP).

The linear approximation (via open system/steady state modeling) of DSi supply are portrayed in Table 1 and Figure 4. Percentage results are relative to the sample that has the highest modeled supply in the record (e.g. 100% at c. 120.5 ka BP; Table 1). Results show an average c. 70% supply (range between c. 64 and c. 100% over the period of MIS 5e) (e.g. c. 30% less supply that at 120.5 ka BP) after the termination of the previous glacial MIS 6 (Figure 4). There is a step increase in modeled supply during MIS 5e, after c. 124.9 ka, which is coincident with the continued decreasing trend in $\delta^{30}Si_{diatom}$ signatures and estimated %DSi utilisation over the course of the Last Interglacial (Figure 4).

Table 1

$\delta^{30}Si_{daitom}$ and $\delta^{29}Si_{daitom}$ data (n=16) reported for the period 132.15 ka BP and 116.16 ka BP, with respective 2σ absolute analytical errors ‰. Sample names are provided in tandem with the modeled respective ages (ka BP) and mid-sediment sampling depth (CON-01-603-2). Data are presented with published total biovolume (millions μm^{-3} cm^{-2} $year^{-1}$) (Rioual and Mackay, 2005) data and the modeled open system %DSi utilsation and Supply (%) for each sample are given.

Sample Name	**Mid-sediment depth (cm)**	**Dating profile (ka BP)**	**$\delta^{30}Si_{diatom}$ (‰)**	**±2s absolute (‰)**	**$\delta^{29}Si_{diatom}$ (‰)**	**±2s absolute (‰)**	**Biovolume** (millions μm^{-3} cm^{-2} $year^{-1}$)	**BVAR Utilisation (%)**	**BVAR Supply (%)**
EEM_12	613	116.16	+1.29	0.09	+0.66	0.04	0.27	73	9
EEM_14	617	117.17	+1.33	0.11	+0.66	0.05	0.18	75	6
EEM_18	625	118.00	+1.40	0.09	+0.73	0.04	1.81	79	59
EEM_20	629	118.42	+1.36	0.10	+0.67	0.04	1.51	76	50
EEM_22	633	118.84	+1.47	0.10	+0.77	0.05	1.39	83	43
EEM_26	641	119.68	+1.31	0.09	+0.68	0.05	1.05	74	36
EEM_30	649	120.53	+1.39	0.11	+0.72	0.04	3.06	78	100
EEM_37	663	122.00	+1.47	0.10	+0.76	0.05	2.21	83	68
EEM_42	673	123.05	+1.48	0.11	+0.80	0.06	1.23	84	38
EEM_48	685	124.32	+1.57	0.08	+0.81	0.06	2.12	90	61
EEM_51	691	124.95	+1.66	0.08	+0.84	0.05	1.56	95	42
EEM_54	697	125.58	+1.69	0.08	+0.85	0.06	1.01	97	27
EEM_58	705	126.42	+1.78	0.11	+0.88	0.06	1.55	102	39
EEM_60	709	126.85	+1.46	0.10	+0.72	0.05	1.02	82	32
EEM_62	713	127.44	+1.77	0.08	+0.90	0.05	0.47	102	12
EEM_73	735	132.15	+1.23	0.09	+0.63	0.05	0.11	68	4

Figure 3.

Stratigraphic plot displaying $\delta^{18}O_{diatom}$ (‰) from Mackay et al. (2013) (note that data before c. 128 ka BP are not plotted due to contamination issues outlined by the authors), $\delta^{30}Si_{diatom}$ (‰) with respective analytical errors, modeled %DSi utilisation from this dataset (open system model), total diatom biovolume accumulation rates (BVAR) (millions μm^{-3} cm^{-2} $year^{-1}$) (Rioual and Mackay, 2005), %BSi (from core BDP-96, Academician Ridge; Prokopenko et al., 2006), dominant diatom species BVAR (thousands/millions μm^{-3} cm^{-2} $year^{-1}$) (Rioual and Mackay, 2005), Chlorophyll *a*/TOC data (µg/mg C; Fietz et al., 2007) and insolation at 55°N (W m^{-2}) for the summer solstice and winter, spring (dashed) equinoxes. All sediment core proxies presented (apart from %BSi) are derived from core CON-01-603-2 (Figure 1).

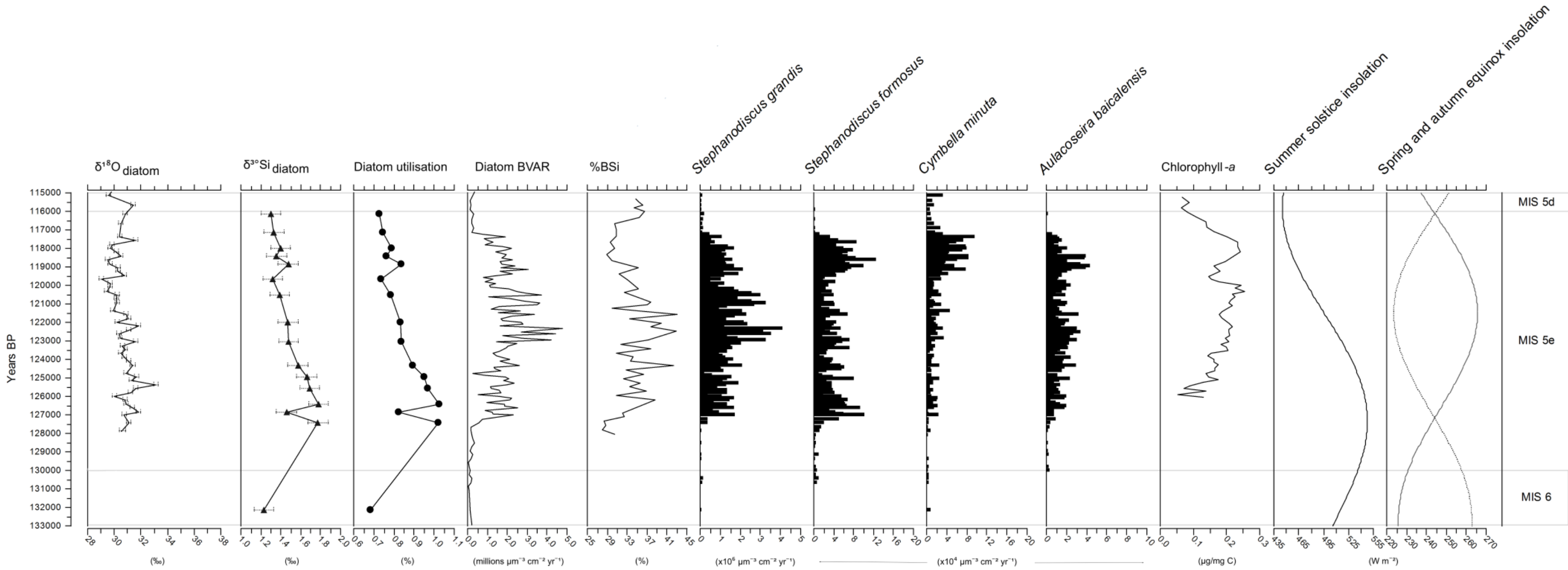

4. Discussion

4.1. $\delta^{30}Si_{diatom}$ signatures during MIS 5e

Although one data point for this record is derived from MIS 6 (before c. 130 ka BP; Table 1, Figure 3), the remainder of the record captures MIS 5e at Lake Baikal and therefore this period acts as the main focus for this discussion. The overall decreasing trend in $\delta^{30}Si_{diatom}$ from c. 127.4 ka BP to c. 116 ka BP, over MIS 5e, is concomitant, and significantly correlated with, the decrease in June (solstice) insolation (at 55°N) (r^2=0.53, p=0.001). However, there is an absence of correlation between $\delta^{30}Si_{diatom}$ and insolation (at 55°N) records of each spring and autumn equinoxes (Figure 3) or winter solstice (data not shown). The range of values presented here (from sediments collected from the North Basin; Figure 1) (+1.23 to +1.78± 0.17‰; Table 1) encompass mean modern day south basin surface sediment $\delta^{30}Si_{diatom}$ signatures (+1.23‰ ± 0.08 1 SD; Panizzo et al., 2016), especially the MIS 6 value. Furthermore, Last Interglacial $\delta^{30}Si_{diatom}$ values (between +1.30 ± 0.10‰ and +1.77 ± 0.08‰; Table 1) are significantly greater than Holocene $\delta^{30}Si_{diatom}$ compositions (Panizzo et al, unpublished data) derived from sediment cores across all three Lake Baikal basins (p=0.001, via a Kruskal Wallis test).

Given the significant greater $\delta^{30}Si_{diatom}$ signatures for MIS 5e we can interpret this as a period of either greater utilisation of DSi by diatoms (e.g. enhanced productivity) and/or a weakened supply of nutrients to the surface (e.g. reduced convective mixing or catchment derived nutrients). The Lake Baikal region was consistently warmer and wetter during the Last Interglacial than the Holocene (Tarasov et al., 2007), which in turn may account for the greater $\delta^{30}Si_{diatom}$-inferred utilisation over this period (Figure 3). These arguments will be discussed further in the following section, in conjunction with other climate and productivity indicators from Lake Baikal during MIS 5e.

Figure 4.

Summary diagram of $\delta^{30}Si_{diatom}$ (‰) with respective analytical errors, modeled %DSi utilisaion and estimated %DSi supply, both constrained by BVAR. S/I ratios and the Hydrolysis Index (note reverse axis) (Fagel et al., 2005), along with dominant catchment biome scores (Tarasov et al., 2005) and summer solstice insolation at 55°N (W m^{-2}). Lines correspond to the time transition from MIS 6 to MIS 5e and MIS 5d. Shaded areas correspond to the interpretation of lake nutrient cycling as described in Section 4.2 and Figure 5 (defined as the DAZ of Rioual and Mackay., 2005).

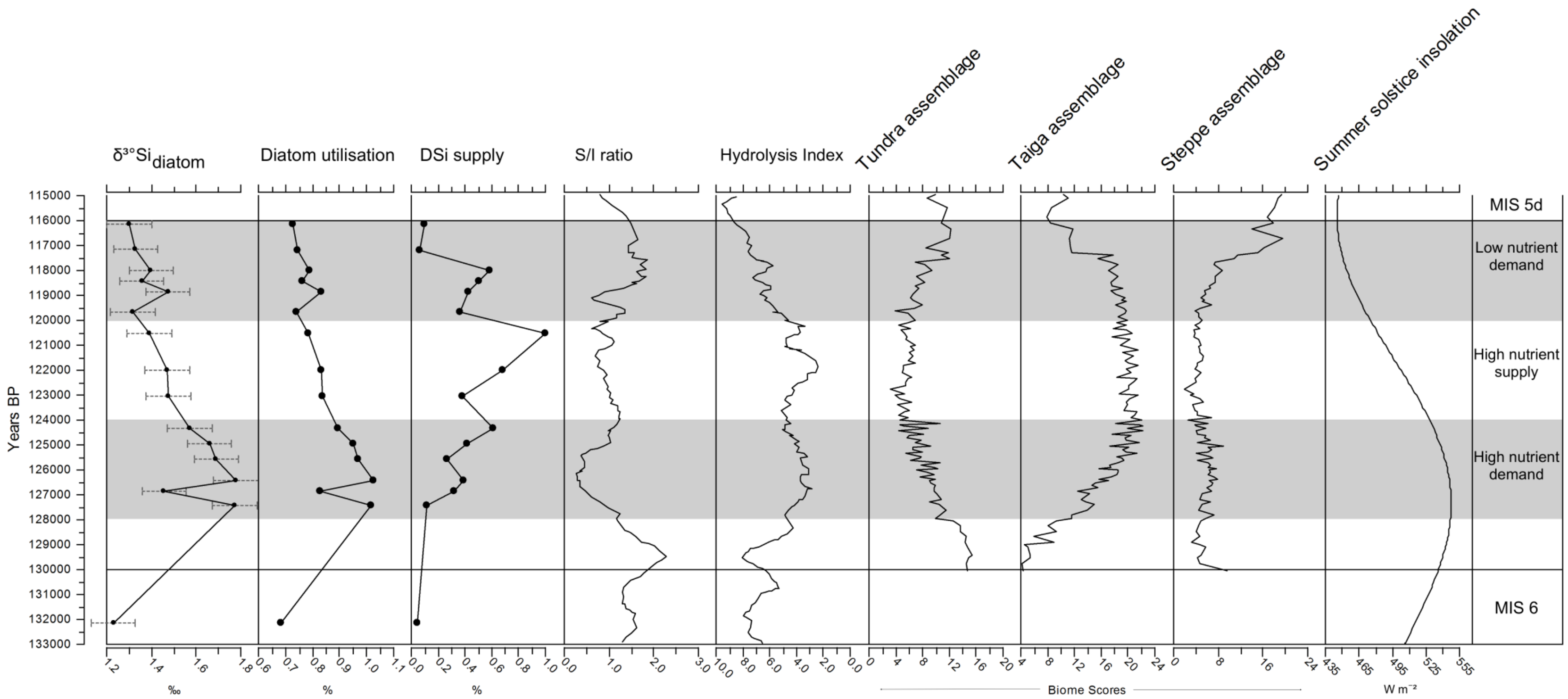

Figure 5. A schematic nutrient-productivity model for the Lake Baikal upper water column (including surface waters to the MMD), during the Last Interglacial. Three interpretive periods are identified (Section 4.2) for MIS 5e and a description of the dominant drivers of upper water column nutrient availability (e.g. catchment versus within-lake) are provided. A summary of the dominant palaeoecological characteristics of these periods is also provided (based on Figures 3, 4), along with the main climatic forcing (e.g. insolation).

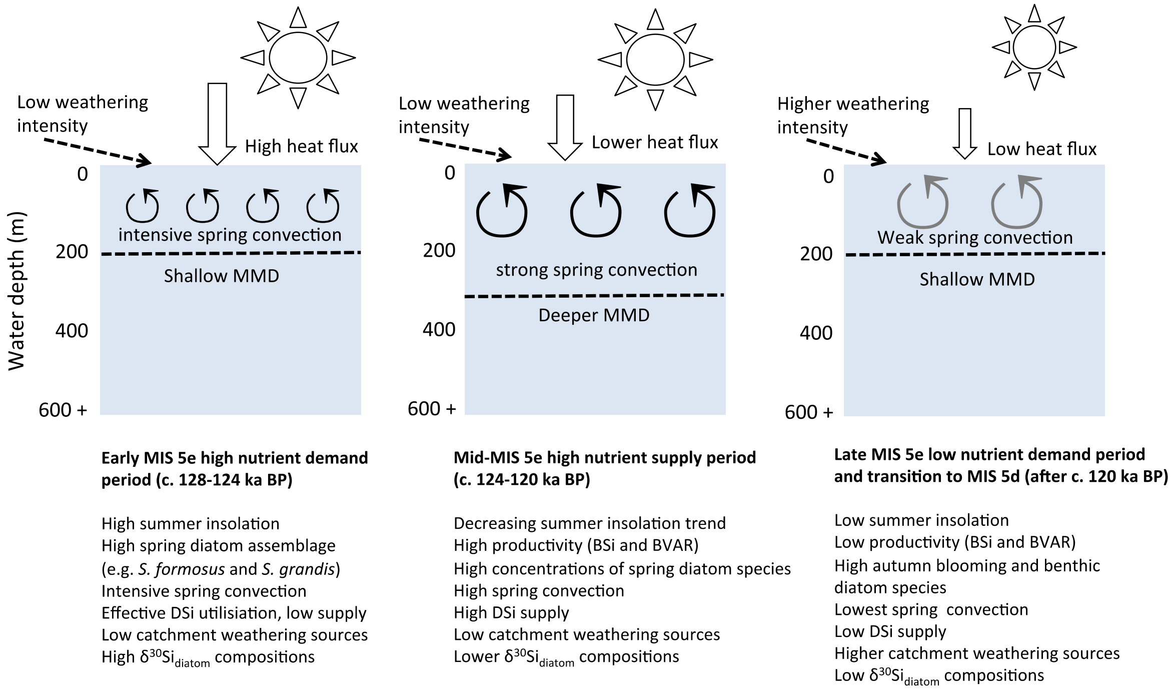

4.2. A conceptual model of diatom responses to altering DSi supply during the Last Interglacial

In the past, a hydrodynamic-insolation model for the Lake Baikal BSi signal was proposed by Prokopenko et al. (2001), where two models were put forward for diatom productivity during either interglacial (high insolation and high BSi) and glacial cycles (low insolation and low BSi). However, as intra-Last Interglacial climate variability has been demonstrated (Karabanov et al., 2000; Mackay et al., 2013; Rioual and Mackay, 2005), we here propose a more sensitive interpretation via the application of diatom BVAR (Section 2.3; Figure 5). This revised nutrient-productivity model reflects the variation captured in both diatom utilisation and nutrient (DSi) supply over the course of MIS 5e (Figure 4), which was otherwise overlooked in earlier models (e.g. Prokopenko et al, 2001).

For the purpose of this discussion, we consider the delivery of nutrients (DSi) from both within-lake (upwelling) and catchment derived processes. The Hydrolosis Index (HI) (Figure 4) of Fagel and Mackay (2008) can be used to examine catchment weathering in the Lake Baikal as a function of climatic conditions, parent rock type and catchment topography (Fagel and Boes, 2008). Higher values therefore indicate the presence of more secondary minerals (e.g. increased weathering), while lower values are indicative of primary mineral clay sources in sediments (e.g. reduced catchment weathering). Furthermore, smectite/illite rations (S/I) are indicative of increased chemical weathering (>1) or increased physical catchment weathering (<1), with illite being defined as one parent mineral endmember for the site (Fagel and Mackay, 2008). In terms of silicon geochemistry, chemical weathering of silicate rocks and minerals are attributable to the DSi load of rivers (and ultimately lakes and oceans)(e.g. Stumm and Wollast, 1990) however, physical erosion (controlled by climate, soil formation and catchment vegetation) can also play an important role in deriving continental DSi fluxes (Gaillardet et al., 1999). Under low erosion rates, weathering is regarded to be supply-limited; so that clay mineral formation is greater (than primary mineral dissolution), which will reduce DSi fluxes (relative to parent material)(e.g. low DSi/[Na+K]*; Fontorbe et al., 2013; Frings et al., 2015; Hughes et al., 2013) and preferentially discriminate against the heavy isotopes (indicative of higher river $\delta^{30}Si_{DSi}$ signatures). This interpretation is referred to as incongruent weathering (refer to the comprehensive discussion of Frings et al., 2016 and references therein). The opposite scenario (kinetic-limited or more congruent weathering) occurs under higher physical erosion rates (e.g. low weathering intensity [W/D]; Bouchez et al., 2014), where the rapid removal of material and low riverine/sedimentary residence times reduces the accumulation of secondary mineral phases (high DSi/[Na+K]*, higher DSi fluxes and lower river $\delta^{30}Si_{DSi}$ signatures).

Quantitative catchment reconstructions of palaeo-weathering fluxes and DSi inflow compositions to Lake Baikal are limited here due to the absence of catchment or riverine endmembers (from MIS 5e). The overall need to expand silicon isotope continental paleo-weathering reconstructions has been highlighted by Frings et al. (2016), although the greatest interest to date centers on quantifying river $\delta^{30}Si_{DSi}$ signature variation to oceans (e.g. continental export) over glacial-interglacial cycles. Given that the global river $\delta^{30}Si_{DSi}$ signatures exported to the ocean, between glacial-interglacial cycles, are modeled to be only small (e.g. estimated globally to increase only c. 0.2 ± 0.25‰ since the Last Glacial Maximum following a reduction in weathering congruency; Frings et al., 2016) it is probable that intra-MIS 5e variability of weathering regimes also has a small impact on altering Lake Baikal source waters over this time. However, we here use the HI and S/I ratio of Fagel and Mackay (2008) as an independent palaeo-weathering proxy to explore this argument and constrain any catchment derived sources of DSi for diatom biomineralisation.

Three descriptive zones (derived from the DAZ of Rioual and Mackay, 2005; shaded in Figure 4) are applied here to examine variations in $\delta^{30}Si_{diatom}$ over the Last Interglacial, as a response to regional climate changes and insolation forcing (Figure 5). We propose that while catchment changes (e.g. biome shifts and weathering rates) may have played a role in regulating catchment DSi supply to Lake Baikal (via rivers) over the course of MIS 5e (Figure 4), these act as more mediated responses. Rather we propose that, as today, within-lake processes (reduced lake ice duration and increased turbulent convective mixing) are more rapid responses to, and therefore act as, the dominant driver in controlling surface waters nutrient change over this time. Below we present a palaeoecological interpretation of the three descriptive zonations (for MIS 5e alone), to which we propose this new interpretation of diatom and nutrient responses over this period (Figure 5).

4.2.1. Early MIS 5e high nutrient demand period (c. 128-124 ka BP):

The increase to higher $\delta^{30}Si_{diatom}$ signatures in MIS 5e (after c. 127.4 ka BP) occurs at peak summer insolation and is also coincident with the increase in diatom BVAR (Rioual and Mackay, 2005) and

BSi records (Prokopenko et al., 2006) and later (after c. 126 ka BP) Chlorophyll-*a* (Figure 3). Mackay et al. (2013) interpret $\delta^{18}O_{diatom}$ data to reflect a period of increased river discharge to Lake Baikal, in response to regional warming (increased pollen-inferred precipitation and temperatures; Tarasov et al., 2007; Tarasov et al., 2005), a weaker Siberian High (Velichko et al., 1991) and teleconnections with the North Atlantic (lowest global ice volume; Kukla et al., 2002; and warmer North Atlantic sea surface temperatures; Oppo et al., 2006). Apart from a brief reduction in $\delta^{30}Si_{diatom}$ signatures to +1.46‰ (± 0.10 2σ) at c. 126.8 ka BP, values otherwise remain high during this period.

Both HI and S/I ratios are low after c. 128 ka BP (after a decreasing trend at the start of MIS 5e; Figure 4), which is indicative of physical (over chemical) weathering processes dominating in the catchment, with limited secondary mineral formation in soils (e.g. low weathering intensity and greater proportion of primary minerals in lake sediments) (Fagel and Mackay, 2008). During this period, these conditions are concomitant with high summer insolation (Figures 4; 5) and an increase in taiga biome scores, indicative of a warming climate (Tarasov et al., 2007; Tarasov et al., 2005). Although the low S/I ratios (the lowest in the record during this period) highlight changes in sediment clay mineralogy, which are a result of soil destabilization in the catchment (Fagel and Mackay, 2008), the low HI is indicative of a low weathering intensity regime in the catchment (with probable low fractionation potential of river waters). This interpretation compares well with BVAR-modeled DSi supply, which is among the lowest of the whole record (40-90% less than peak supply at c. 120.5 ka BP; Table 1). Taken together these data suggest that the magnitude of change to catchment DSi source waters was not great enough to considerably alter $\delta^{30}Si_{initial}$, so that the high $\delta^{30}Si_{diatom}$ signatures are driven more strongly by diatom biomineralisation.

During the "high nutrient demand period" (c. 128 to 124 ka BP), spring blooming species *Stephanodiscus formosus* and *Stephaniodiscus grandis* (the latter which contributes the greatest to diatom BVAR; Figure 3) also increase, along with other planktonic endemic *Aulacoseira baicalensis* and *Aulacoseira skvortzowii* species (Rioual and Mackay, 2005). Although these *Stephanodiscus* species are today extinct, based on modern analogues, Rioual and Mackay (2005) attribute them to be slow growing due to their large size, existing in low light conditions with a high phosphorous and moderate silica demand, associated today with long deep convective spring mixing (up tp 300 m;

Shimaraev et al., 1993). These data point to the interpretation of enhanced nutrient exchange in surface waters at the beginning of MIS 5e, and a productive initial spring diatom bloom, dominated by the high phosphorous, moderate DSi, nutrient demand *Stephanodiscus* species (Figures 3,4). With low-modeled DSi supply over this period (including from catchment sources), $\delta^{30}Si_{diatom}$ compositions become more enriched with an overall switch to greater diatom productivity (%BSi, BVAR; Figures 3, 4) and DSi utilisation.

4.2.2. Mid-MIS 5e high nutrient supply period (c. 124-120 ka BP)

After c. 124 ka BP lower estimations of DSi utlisation are seen, with more nutrient rich conditions (concomitant with the decreasing trend in $\delta^{30}Si_{diatom}$ signatures and step shift in higher diatom BVAR) (Figure 4). This trend also follows the decreasing summer insolation and $\delta^{18}O_{diatom}$ compositions (Figures 3, 4), although the catchment is composed of a stable taiga biome (Figure 4; Tarasov et al., 2007; Tarasov et al., 2005). Clay mineralogy (S/I ratio) during this zone continues to suggest conditions indicative of physical (over chemical) weathering, with sediments dominated by primary mineral sources (low HI; Figure 4) and therefore low chemical weathering in the catchment over this period. We interpret the record therefore to point to a continued low weathering intensity (Section 4.2.1). As Lake Baikal catchment conditions appear relatively stable during this zone (based on pollen and clay mineralogy) but modeled DSi supply increases (Figure 4), we attribute this to mean that within-lake DSi sources (e.g. increased mixing) are more important in driving lower $\delta^{30}Si_{diatom}$ signatures (i.e. increased supply versus reduced diatom uptake) rather than an increased catchment derived source of DSi (e.g. of lower $\delta^{30}Si_{DSi}$ composition).

Estimated supply increases during this period (c. 124 to 120 ka BP) reaching the time of highest modeled supply (100%) at 120.5 ka BP (Table 1), concomitant with highest diatom BVAR and increased Chlorophyll-*a* concentrations (Fietz et al., 2007) and %BSi (Prokopenko et al., 2006)(Figure 3). The increase in diatom BVAR is again attributed to the increase in *S. grandis* species (Rioual and Mackay, 2005), which proportionally dominates diatom biovolumes over MIS 5e. We propose (based on modern-analogue diatom ecology) a shift towards a deeper mesothermal maximum depth (MMD; Figure 5), concomitant with a deeper spring mixing layer compared to the previous period. This will account for the increase in DSi supply to surface waters and therefore some of the lowest $\delta^{30}Si_{diatom}$ compositions in the reconstruction, despite increased diatom productivity.

4.2.3 Low nutrient demand period and the transition to MIS 5d (after 120 ka BP)

After c. 120.4 ka BP Rioual and Mackay (2005) document a notable change in individual diatom species BVAR at Lake Baikal, from the large-celled *Stephanodiscus* species (particularly *S. grandis* which dominates the overall proportion of total biovolumes) to smaller celled *Cyclotella* species, especially *Cyclotella minuta* (Figures 3; 5). *C. minuta* can tolerate relatively high summer surface water temperatures (e.g. during stratification), so that when autumnal mixing begins they are among the first species to bloom (Jewson et al., 2015). These species changes are concomitant with a stepwise decrease in both %BSi and total diatom BVAR, which points to a decrease in overall diatom productivity in Lake Baikal (Figure 3). Decreasing $\delta^{30}Si_{diatom}$ compositions and modeled DSi utilisation may further corroborate this reduction in productivity, leading to the interpretation of reduced DSi demand (due to both reduced productivity and the prevalence of smaller diatom species) along with low $\delta^{30}Si_{diatom}$ compositions and modeled DSi supply (Figure 5). Overall we propose conditions less favorable for larger spring blooming species (e.g. *S. grandis*). In particular, overall reduced productivity is attributed to weaker spring convective mixing, the breakdown in thermal driven stratification and a reduction in the overall growing season (increased ice cover duration) consistent with the move to cooler conditions in the region (Figure 5).

Superimposed on these trends is a minimum in $\delta^{18}O_{diatom}$ compositions between c. 120.5 and 119.7 ka BP (Figure 3), which Mackay et al. (2013) attribute to a cold perturbation in the Lake Baikal region (an increase in Siberian High intensity; Tarasov et al., 2005) with increased snowmelt contributions and a reduction in primary productivity (Fietz et al., 2007; Prokopenko et al., 2006; Rioual and Mackay, 2005). Similarly, $\delta^{30}Si_{diatom}$ signatures also show a small decline (although within analytical uncertainty), which could be reflecting reduced diatom productivity during this cold event and therefore low DSi uptake (and low modeled DSi supply) (Figures 4, 5). Interestingly, S/I ratios and HI increase after c. 120 ka BP (Figure 4), which points to an increase in chemical weathering (intensity) in the Lake Baikal catchment (e.g. towards supply-limited weathering regimes, indicative of higher river $\delta^{30}Si_{DSi}$), although as there are no large changes in $\delta^{30}Si_{diatom}$ compositions after this time, we again suggest that isotopically altered source waters to the lake have not had a confounding impact in driving $\delta^{30}Si_{diatom}$ signatures after this time.

After c. 117.2 ka BP benthic diatom species increase in relative abundance (Rioual and Mackay, 2005). This, along with a sharp fall in %BSi (Prokopenko et al., 2006) and Chlorophyll-*a* concentrations (Fietz et al., 2007), points to a reduction in pelagic productivity indicative of a switch to a much colder climate, coincident with a continued decline in summer insolation, a shift to increased steppe biome scores (Figure 4) and reduced mean summer temperatures (Tarasov et al., 2007; Tarasov et al., 2005), all while ice sheet growth occurred in the Northern Hemisphere (Kukla et al., 2002).

5. Conclusions

We present the first application of $\delta^{30}Si_{diatom}$ in the palaeorecord at Lake Baikal and present it as a proxy for both nutrient availability and demand over the Last Interglacial (MIS 5e). Overall, diatom productivity is significantly greater in MIS 5e compared to the Holocene. In tandem with other published productivity indicators from core CON-01-603-2, data point to an early interglacial stage of high DSi demand by diatoms although low nutrient conditions, in response to regional climate warming, catchment vegetation and weathering regime changes. After c. 124 ka BP data suggest a move to greater nutrient supply, although we attribute this to an increase in spring convective mixing based on overall reconstructions of a stable Lake Baikal catchment (e.g. weathering indices and vegetation). We propose complex within-lake conditions over the duration of MIS 5e, based on the variability in diatom nutrient uptake and surface water nutrient availability (e.g. driven by changes in lake ice duration and turbulent convective mixing). Unlike the earlier interpretative palaeoproductivity models based on BSi data alone, we derive a more nuanced reconstruction highlighting that more caution should be taken to better understand the mechanisms at play both inter- and intra-interglacial/glacial climates. This will better inform the sensitivity and response of Lake Baikal to climate change both in the past and under future anthropogenic and climate pressures.

Acknowledgements:

This project was funded by National Environmental Research Council (NERC) Standard Grants NE/J00829X/1, AWM acknowledges contributions from the EU FPV Project "CONTINENT" (Ref: EKV2-2000-00057), for funding previous Last Interglacial studies on Lake Baikal.

References:

Alleman, L.Y., Cardinal, D., Cocquyt, C., Plisnier, P.D., Descy, J.P., Kimirei, I., Sinyinza, D., André, L., 2005. Silicon isotopic fractionation in Lake Tanganyika and its main tributaries. J. Great Lakes Res. 31, 509-519

Bouchez, J., Gaillardet, J., F, v.B., 2014. Weathering intensity in lowland river basins: from the Andes to the Amazon mouth. Procedia Earth Planetary Sciences 10, 280-286

Cardinal, D., Alleman, L.Y., de Jong, J., Ziegler, K., Andre, L., 2003. Isotopic composition of silicon measured by multicollector plasma source mass spectrometry in dry plasma mode. J. Anal. At. Spectrom. 18, 213-218. doi: 10.1039/B210109b

Charlet, F., Fagel, N., De Batist, M., Hauregard, F., Minnebo, B., Meischner, D., Team, S., 2005. Sedimentary dynamics on isolated highs in Lake Baikal: evidence from detailed high-resolution geophysical data and sediment cores. Global Planet. Change 46, 125-144. doi: 10.1016/J.Gloplacha.2004.11.009

De La Rocha, C.L., Brzezinski, M.A., DeNiro, M.J., 1997. Fractionation of silicon isotopes by marine diatoms during biogenic silica formation. Geochim. Cosmochim. Acta 61, 5051-5056. doi: 10.1016/s0016-7037(97)00300-1

Demarest, M.S., Brzezinski, M.A., Beucher, C.P., 2009. Fractionation of silicon isotopes during biogenic silica dissolution. Geochim. Cosmochim. Acta 73, 5572-5583. doi:10.1016/j.gca.2009.06.019

Demory, F., Nowaczyk, N.R., Witt, A., Oberhansli, H., 2005a. High-resolution magneto stratigraphy of late quaternary sediments from Lake Baikal, Siberia: timing of intracontinental paleoclimatic responses. Global Planet. Change 46, 167-186. doi: 10.1016/j.gloplacha.2004.09.016

Demory, F., Oberhansli, H., Nowaczyk, N.R., Gottschalk, M., Wirth, R., Naumann, R., 2005b. Detrital input and early diagenesis in sediments from Lake Baikal revealed by rock magnetism. Global Planet. Change 46, 145-166. doi:10.1016/j.gloplacha.2004.11.010

Dodson, S.I., Arnott, S.W., Cottingham, K.L., 2000. The relationship in lake communities between primary productivity and species richness. Ecology 81, 2662-2679

Fagel, N., Alleman, L.Y., Granina, L., Hatert, F., Thamo-Bozso, E., Cloots, R., Andre, L., 2005. Vivianite formation and distribution in Lake Baikal sediments. Global Planet. Change 46, 315-336. doi: 10.1016/J.Gloplacha.2004.09.022

Fagel, N., Boes, X., 2008. Clay-mineral record in Lake Baikal sediments: The Holocene and Late Glacial transition. Palaeogeography Palaeoclimatology Palaeoecology 259, 230-243. doi:10.1016/j.palaeo.2007.10.009

Fagel, N., Mackay, A.W., 2008. Weathering in the Lake Baikal watershed during the Kazantsevo (Eemian) interglacial: Evidence from the lacustrine clay record. Palaeogeography Palaeoclimatology Palaeoecology 259, 244-257. doi: 10.1016/J.Palaeo.2007.10.011

Fietz, S., Nicklisch, A., Oberhansli, H., 2007. Phytoplankton response to climate changes in Lake Baikal during the Holocene and Kazantsevo Interglacials assessed from sedimentary pigments. J. Paleolimnol. 37, 177-203. doi: 10.1007/s10933-006-9012-y

Fontorbe, G., De La Rocha, C.L., Chapman, H.J., Bickle, M.J., 2013. The silicon isotopic composition of the Ganges and its tributaries. Earth. Planet. Sci. Lett. 381, 21-30. doi: 10.1016/J.Epsl.2013.08.026

Frings, P.J., Clymans, W., Fontorbe, G., De La Rocha, C.L., Conley, D.J., 2016. The continental Si cycle and its impact on the ocean Si isotope budget. Chem. Geol. 425, 12-36. doi: 10.1016/j.chemgeo.2016.01.020

Frings, P.J., Clymans, W., Fontorbe, G., Gray, W., Chakrapani, G.J., Conley, D.J., De La Rocha, C., 2015. Silicate weathering in the Ganges alluvial plain. Earth. Planet. Sci. Lett. 427, 136-148. doi:10.1016/j.epsl.2015.06.049

Fripiat, F., Cavagna, A.J., Dehairs, F., Speich, S., Andre, L., Cardinal, D., 2011. Silicon pool dynamics and biogenic silica export in the Southern Ocean inferred from Si-isotopes. Ocean Sci. 7, 533-547. doi:10.5194/os-7-533-2011

Gaillardet, J., Dupré, B., Louvat, P., Allègre, C.J., 1999. Global silicate and CO_2 consumption rates deduced from the chemistry of large rivers. Chem. Geol. 159, 3-30

Georg, R.B., Reynolds, B.C., Frank, M., Halliday, A.N., 2006. New sample preparation techniques for the determination of Si isotopic compositions using MC-ICP-MS. Chem. Geol. 235, 95-104. doi: 10.1016/J.Chemgeo.2006.06.006

Granoszewski, W., Demske, D., Nita, M., Heumann, G., Andreev, A., 2005. Vegetation and climatic variability during the Last interglacial evidenced in the pollen record from Lake Baikal. Global Planet. Change 46, 187-198

Horn, M.G., Beucher, C.P., Robinson, R.S., Brzezinski, M.A., 2011. Southern ocean nitrogen and silicon dynamics during the last deglaciation. Earth. Planet. Sci. Lett. 310, 334-339. doi: 10.1016/j.epsl.2011.08.016

Hughes, H.J., Delvigne, C., Korntheuer, M., de Jong, J., André, L., Cardinal, D., 2011. Controlling the mass bias introduced by anionic and organic matrices in silicon isotopic measurements by MC-ICP-MS. J. Anal. At. Spectrom. 26, 1892-1896. doi: 10.1039/C1ja10110b

Hughes, H.J., Sondag, F., Santos, R.V., Andre, L., Cardinal, D., 2013. The riverine silicon isotope composition of the Amazon Basin. Geochim. Cosmochim. Acta 121, 637-651. doi: 10.1016/j.gca.2013.07.040

Jewson, D.H., Granin, N.G., Gnatovsky, R.Y., Lowry, S.F., Teubner, K., 2015. Coexistence of two *Cyclotella* diatom species in the plankton of Lake Baikal. Freshwat. Biol. 60, 2113-2126. doi: 10.1111/fwb.12636

Karabanov, E., Prokopenko, A.A., Williams, D., Khursevich, G., 2000. Evidence for mid-Eemian cooling in continental climatic record from Lake Baikal. J. Paleolimnol. 23, 365-371

Kukla, G.J., Bender, M.L., de Beaulieu, J.L., Bond, G., Broecker, W.S., Cleveringa, P., Gavin, J.E., Herbert, T.D., Imbrie, J., Jouzel, J., Keigwin, L.D., Knudsen, K.L., McManus, J.F., Merkt, J., Muhs, D.R., Muller, H., Poore, R.Z., Porter, S.C., Seret, G., Shackleton, N.J., Turner, C., Tzedakis, P.C., Winograd, I.J., 2002. Last interglacial climates. Quatern. Res. 58, 2-13. doi: 10.1006/qres.2002.2316

Lydolph, P.E., 1977. Geography of the USSR. Elsevier, The Hague.

Mackay, A., 2007. The paleoclimatology of Lake Baikal: A diatom synthesis and prospectus. Earth Science Reviews 82, 181-215

Mackay, A.W., Swann, G.E.A., Fagel, N., Fietz, S., Leng, M.J., Morley, D., Rioual, P., Tarasov, P., 2013. Hydrological instability during the Last Interglacial in central Asia: a new diatom oxygen isotope record from Lake Baikal. Quaternary Science Reviews 66, 45-54. doi: 10.1016/j.quascirev.2012.09.025

Martin-Jezequel, V., Hildebrand, M., Brzezinski, M.A., 2000. Silicon metabolism in diatoms: Implications for growth. J. Phycol. 36, 821-840. doi: 10.1046/J.1529-8817.2000.00019.X

Milligan, A.J., Varela, D.E., Brzezinski, M.A., Morel, F.O.M.M., 2004. Dynamics of silicon metabolism and silicon isotopic discrimination in a marine diatom as a function of $p\mathrm{CO_2}$. Limnol. Oceanogr. 49, 322-329

Morley, D.W., Leng, M.J., Mackay, A.W., Sloane, H.J., Rioual, P., Sturm, M., 2004. Cleaning of lake sediment samples for diatom oxygen isotope analysis. J. Paleolimnol. 31, 391-401

Opfergelt, S., Eiriksdottir, E.S., Burton, K.W., Einarsson, A., Siebert, C., Gislason, S.R., Halliday, A.N., 2011. Quantifying the impact of freshwater diatom productivity on silicon isotopes and silicon fluxes: Lake Myvatn, Iceland. Earth. Planet. Sci. Lett. 305, 73-82. doi: 10.1016/j.epsl.2011.02.043

Oppo, D.W., McManus, J.F., Cullen, J.L., 2006. Evolution and demise of the Last Interglacial warmth in the subpolar North Atlantic. Quaternary Science Reviews 25, 3268-3277. doi: 10.1016/j.quascirev.2006.07.006

Panizzo, V.N., Roberts, S., Swann, G.A.A., McGowan, S., Mackay, A.W., Vologina, E., Pashley, V., Horstwood, M.S.A., In review. Spatial differences in dissolved silicon utilisation in Lake Baikal, Siberia: disentangling the effects of high diatom biomass events and eutrophication. Limnol. Oceanogr.

Panizzo, V.N., Swann, G.E., Mackay, A.W., Vologina, E.G., Pashley, V.H., Horstwood, M.S.A., 2017. Constraining modern-day silicon cycling in Lake Baikal. Global Biogeochem. Cycles 2017, 556-574. doi: 10.1002/2016GB005518

Panizzo, V.N., Swann, G.E.A., Mackay, A.W., Vologina, E., Sturm, M., Pashley, V., Horstwood, M.S.A., 2016. Insights into the transfer of silicon isotopes into the sediment record. Biogeosciences 13, 147-157. doi: 10.5194/bg-13-147-2016

Past Interglacials Working Group of PAGES., 2016. Interglacials of the last 800,000 years. 54, 162-219. doi:10.1002/2015RG000482

Popovskaya, G.I., 2000. Ecological monitroing of phytoplankton in Lake Baikal. Aquat. Ecosyst. Health Manage. 3, 215-225

Popovskaya, G.I., Usol'tseva, M.V., Domysheva, V.M., Sakirko, M.V., Blinov, V.V., Khodzher, T.V., 2015. The Spring Phytoplankton in the Pelagic Zone of Lake Baikal During 2007-2011. Geogr. Natural Resources 36, 253-262. doi: 10.1134/s1875372815030051

Prokopenko, A.A., Hinnov, L.A., Williams, D.F., Kuzmin, M.I., 2006. Orbital forcing of continental climate during the Pleistocene: a complete astronomically tuned climatic record from Lake Baikal, SE Siberia. Quaternary Science Reviews 25, 3431-3457. doi: 10.1016/j.quascirev.2006.10.002

Prokopenko, A.A., Karabanov, E.B., Williams, D.F., Kuzmin, M.I., Shackleton, N.J., Crowhurst, S.J., Peck, J.A., Gvozdkov, A.N., King, J.W., 2001. Biogenic silica record of the Lake Baikal response to climatic forcing during the Brunhes. Quatern. Res. 55, 123-132. doi: 10.1006/qres.2000.2212

Railsback, L.B., Gibbard, P.L., Head, M.J., Voarintsoa, N.R.G., Toucanne, S., 2015. An optimized scheme of lettered marine isotope substages for the last 1.0 million years, and the climatostratigraphic nature of isotope stages and substages. Quaternary Science Reviews 111, 94-106. doi: 10.1016/j.quascirev.2015.01.012

Reynolds, B.C., Aggarwal, J., Andre, L., Baxter, D., Beucher, C., Brzezinski, M.A., Engström, E., Georg, R.B., Land, M., Leng, M.J., Opfergelt, S., Rodushkin, I., Sloane, H., van den Boorn, S.H.J.M., Vroon, P.Z., Cardinal, D., 2007. An inter-laboratory comparison of Si isotope reference materials. J. Anal. At. Spectrom. 22, 561-568

Rioual, P., Mackay, A.W., 2005. A diatom record of centennial resolution for the Kazantsevo Interglacial stage in Lake Baikal (Siberia). Global Planet. Change 46, 199-219. doi: 10.1016/j.gloplacha.2004.08.002

Ryves, D.B., Jewson, D.H., Sturm, M., Battarbee, R.W., Flower, R.J., Mackay, A.W., Granin, N.G., 2003. Quantitative and qualitative relationships between planktonic diatom communities and diatom assemblages in sedimenting material and surface sediments in Lake Baikal, Siberia. Limnol. Oceanogr. 48, 1643-1661

Shimaraev, M.N., Granin, N.G., Zhdanov, A.A., 1993. Deep ventilation of Lake Baikal waters due to spring thermal bars. Limnological and Oceanography 38, 1068-1072

Short, D.A., Mengel, J.G., Crowley, T.J., Hyde, W.T., North, G.R., 1991. Filtering of Milankovitch Cycles by Earths Geography. Quatern. Res. 35, 157-173. doi: 10.1016/0033-5894(91)90064-C

Stumm, W., Wollast, R., 1990. Coordination chemistry of weathering: kinetics of the surface-controlled dissolution of oxide minerals. Review of Geophysics 28, 53-69

Sun, X.L., Andersson, P.S., Humborg, C., Pastuszak, M., Morth, C.M., 2013. Silicon isotope enrichment in diatoms during nutrient-limited blooms in a eutrophied river system. Journal of Geochemical Exploration 132, 173-180. doi: 10.1016/J.Gexplo.2013.06.014

Sutton, J.N., Varela, D.E., Brzezinski, M.A., Beucher, C.P., 2013. Species-dependent silicon isotope fractionation by marine diatoms. Geochim. Cosmochim. Acta 104, 300-309. doi: 10.1016/J.Gca.2012.10.057

Tarasov, P., Bezrukova, E., Karabanov, E., Nakagawa, T., Wagner, M., Kulagina, N., Letunova, P., Abzaeva, A., Granoszewski, W., Riedel, F., 2007. Vegetation and climate dynamics during the Holocene and Eemian interglacials derived from Lake Baikal pollen records. Palaeogeography, Palaeoclimatology, Palaeoecology 252, 440-457. doi: 10.1016/j.palaeo.2007.05.002

Tarasov, P., Granoszewski, W., Berzukova, Y.V., Brewer, S., Nita, M., Abzaeva, A., Oberhaensli, H., 2005. Quantitative reconstruction of the Last Interglacial climate based on the pollen record from Lake Baikal, Russia. Clim. Dyn. 25, 625-637

Varela, D.E., Pride, C.J., Brzezinski, M.A., 2004. Biological fractionation of silicon isotopes in Southern Ocean surface waters. Global Biogeochem. Cycles 18. doi: 10.1029/2003gb002140

Velichko, A.A., Borisova, O.K., Gurtovaya, Y.Y., Zelikson, E.M., 1991. Climatic rhythm of the last interglacial in northern Eurasia. Quaternary International 10-12, 191-213

Williams, D.F., Kuzmin, M.I., Prokopenko, A.A., Karabanov, E.B., Khursevich, G.K., Bezrukova, E.V., 2001. The Lake Baikal drilling projects in the context of a global lake drilling initiative. Quaternary International 80-1, 3-18. doi: 10.1016/S1040-6182(01)00015-5

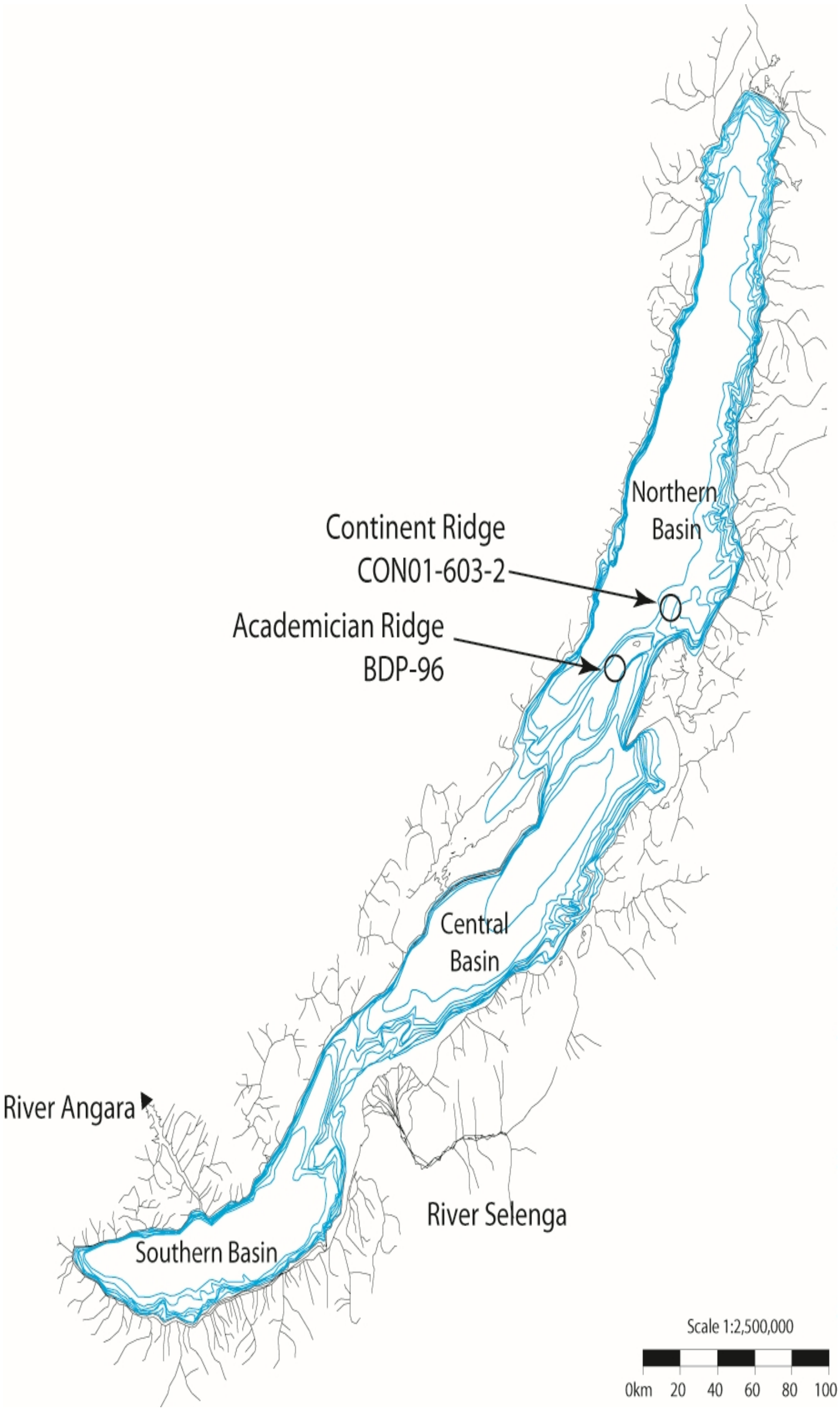
Northern Basin
Continent Ridge
CON01-603-2
Academician Ridge
BDP-96
Central Basin
River Angara
River Selenga
Southern Basin
Scale 1:2,500,000
0km 20 40 60 80 100

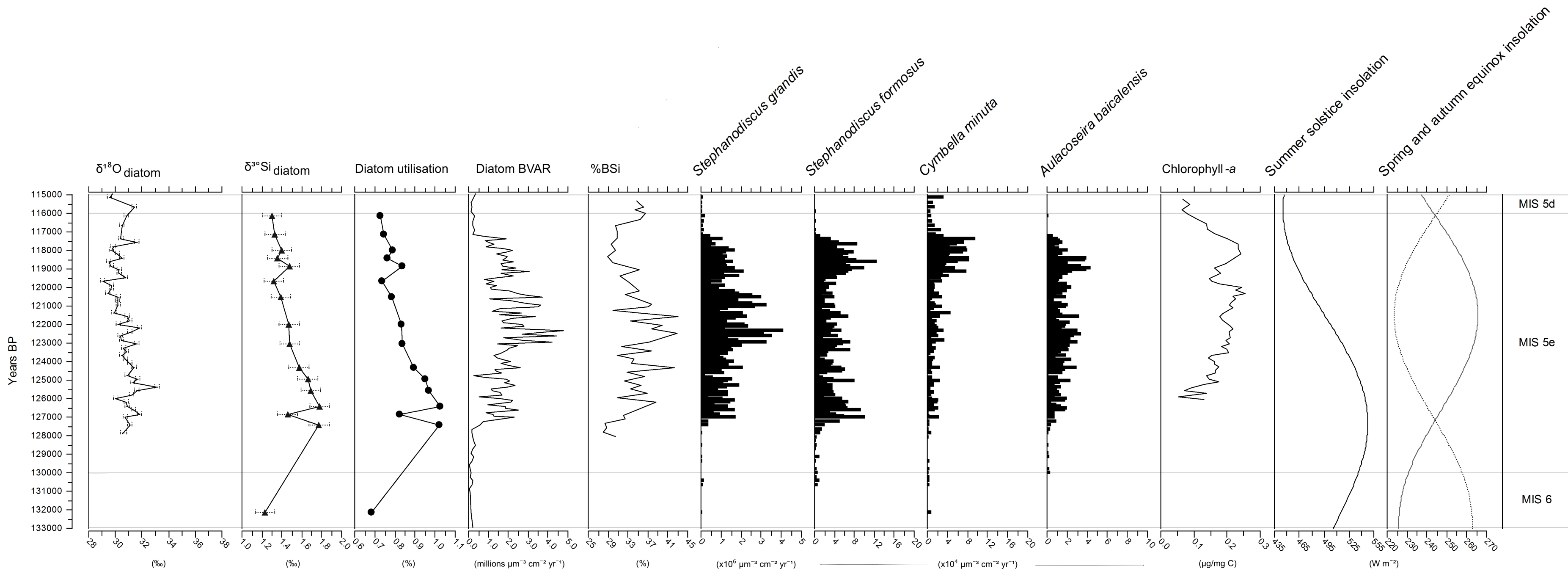

δ18O diatom
δ30Si diatom
Diatom utilisation
Diatom BVAR
%BSi
Stephanodiscus grandis
Stephanodiscus formosus
Cymbella minuta
Aulacoseira baicalensis
Chlorophyll-a
Summer solstice insolation
Spring and autumn equinox insolation
Years BP
MIS 5d
MIS 5e
MIS 6
(‰)
(‰)
(%)
(millions µm⁻³ cm⁻² yr⁻¹)
(%)
(x10⁶ µm⁻³ cm⁻² yr⁻¹)
(x10⁴ µm⁻³ cm⁻² yr⁻¹)
(µg/mg C)
(W m⁻²)

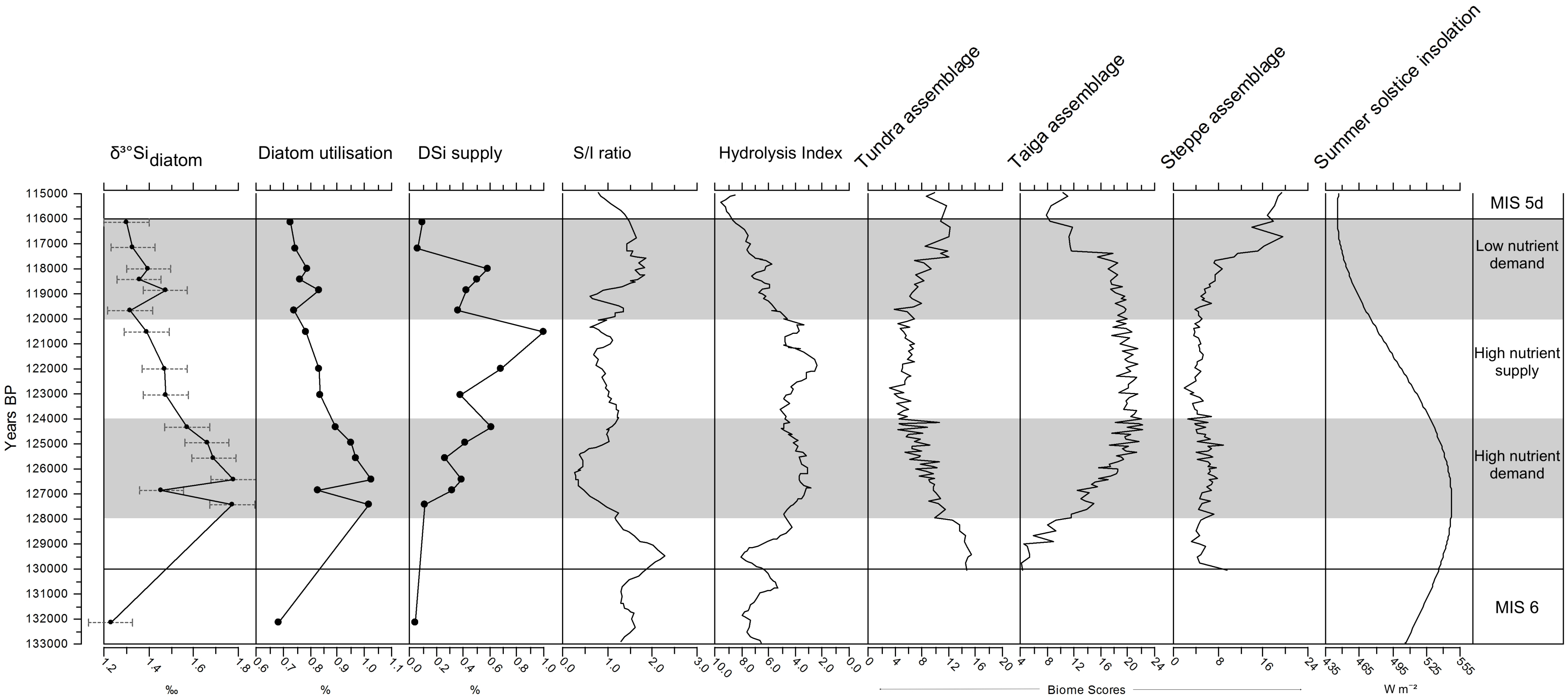

δ30Si diatom
Diatom utilisation
DSi supply
S/I ratio
Hydrolysis Index
Tundra assemblage
Taiga assemblage
Steppe assemblage
Summer solstice insolation
Years BP
MIS 5d
Low nutrient demand
High nutrient supply
High nutrient demand
MIS 6
‰
%
%
Biome Scores
W m⁻²

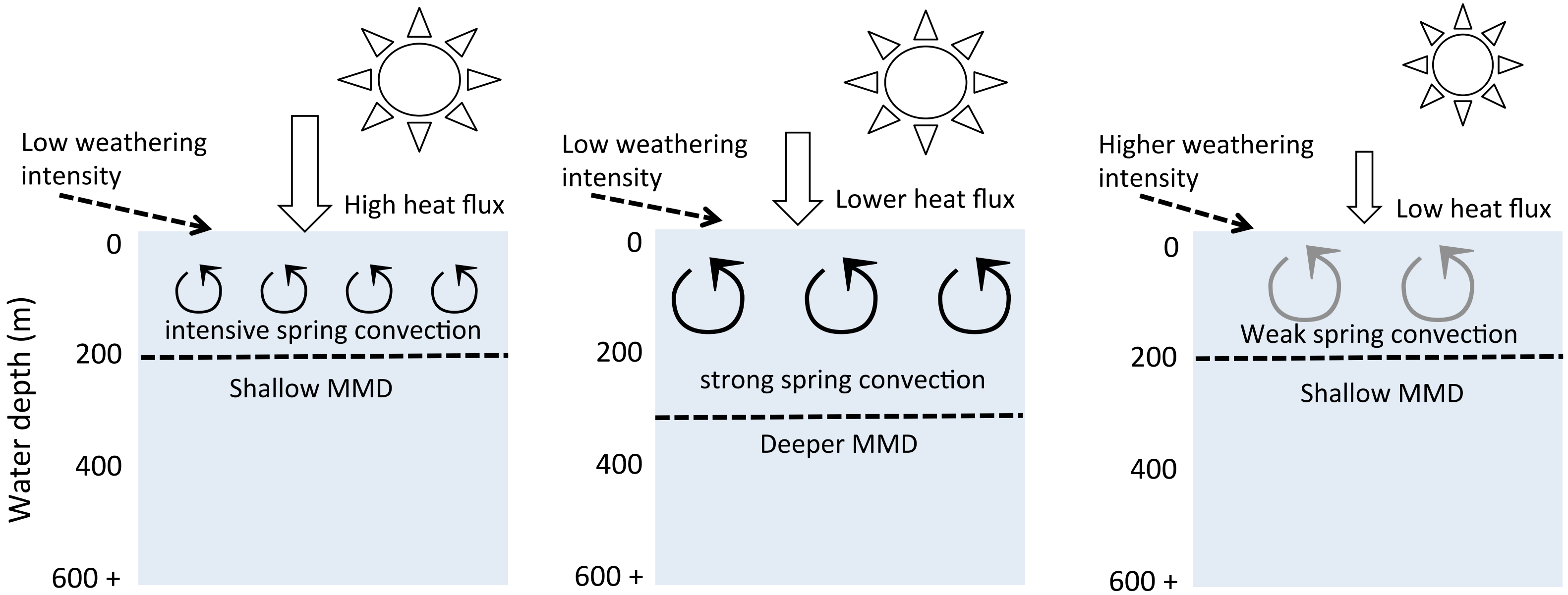

Early MIS 5e high nutrient demand period (c. 128-124 ka BP)

High summer insolation
High spring diatom assemblage
(e.g. *S. formosus* and *S. grandis*)
Intensive spring convection
Effective DSi utilisiation, low supply
Low catchment weathering sources
High $\delta^{30}Si_{diatom}$ compositions

Mid-MIS 5e high nutrient supply period (c. 124-120 ka BP)

Decreasing summer insolation trend
High productivity (BSi and BVAR)
High concentrations of spring diatom species
High spring convection
High DSi supply
Low catchment weathering sources
Lower $\delta^{30}Si_{diatom}$ compositions

Late MIS 5e low nutrient demand period and transition to MIS 5d (after c. 120 ka BP)

Low summer insolation
Low productivity (BSi and BVAR)
High autumn blooming and benthic diatom species
Lowest spring convection
Low DSi supply
Higher catchment weathering sources
Low $\delta^{30}Si_{diatom}$ compositions